Transactions, SMiRT-26
Berlin/Potsdam, Germany, July 10-15, 2022
Division I

BOND BEHAVIOUR AND CRACK PROPAGATION OF REINFORCED CONCRETE UNDER LONG-TERM LOADING

Marc Koschemann[1], Manfred Curbach[2]

[1] Dipl.-Ing., Institute of Concrete Structures, Dresden (marc.koschemann@tu-dresden.de.)
[2] Prof. Dr.-Ing. Dr.-Ing. E.h., Institute of Concrete Structures, Dresden

ABSTRACT

Cracks are part of every reinforced concrete component and affect the durability and serviceability of those. The crack width may grow under long-time loading, which is mainly caused by bond creep. Current investigations at the Technische Universität Dresden focus on the bond behaviour and the bond stress distribution of ribbed steel bars under long-term loading. Different kinds of concrete are used, reaching from a mean uniaxial strength of f_{cm} = 30 MPa up to f_{cm} = 70 MPa. The experimental program includes systematic investigations of the influence of the bond length on the ultimate bond stress using pull-out tests and beam-end tests as well. In addition, tension tie tests under sustainable loading are conducted, the results of which will be used to validate calculated crack widths. The bond behaviour is detected by displacement transducers and fibre-optic sensors, which enable the quasi-continuous recording of strain. Based on the local resolution of the strain along an embedded steel bar, conclusions about the force transmission between reinforcement and concrete are made.

This article deals with the experimental and instrumental setup, results of the first test series and the procedure of evaluation. Furthermore, the results are compared to existing bond models and the influence of the test specimen and the bond length are discussed.

INTRODUCTION

Background

For critical infrastructure buildings such as hospitals, government buildings, nuclear power plants as well as interim and final storage facilities for radioactive material, there is a need for special protection of these buildings. Especially in the context of the foreseeable significantly extended interim storage periods for nuclear waste (see e.g. BASA (2019) and BMWi (2018)), the question arises as to how this long-term exposure affects the structural integrity and durability of existing building structures. The evaluation of this requires precise knowledge of crack formation processes and crack width development of reinforced concrete. Cracks belong to the material reinforced concrete and are necessary for its load-bearing mechanism. However, cracks are the weak points of reinforced concrete components and can be the cause of leaks and corrosion of the reinforcing steel and thus lead to a deterioration of the durability, serviceability and load-bearing capacity of reinforced concrete structures. The cracking behaviour is significantly influenced by the bonding effect between reinforcing steel and concrete. Therefore, a comprehensive understanding of bond effects, including the local and time-dependant stress distribution along the reinforcement bar, is necessary for the design and evaluation of structural elements in nuclear and interim storage facilities.

Principles and testing of bond behaviour

Since the beginning of research on reinforced concrete, efforts have been made to quantify the bonding effect between reinforcing bar and concrete. To describe the bond behaviour, the relationship between the bond stress τ as the sum of the individual bond mechanisms, adhesion, friction and mechanical interaction, and the relative displacement, the so-called slip s_0, is used. For the experimental determination of this relationship, bond tests are carried out, where the bond stress is the pull-out force F related to the bond area A_b (1).

$$\tau = \frac{F}{A_b} = \frac{\sigma_s \cdot d_s}{4 \cdot l_b} \tag{1}$$

However, according to Lindorf (2011), more than 30 parameters influence the bond behavior in the experiment. In addition to the material and geometry properties of the concrete and the bar as well as the type of loading, also the test setup or specimen play a major role in this. Thus, different test specimens result in different bond stress-slip relationships. The most used test to evaluate the bond behaviour of steel reinforcement is the pull-out test (PO) according to RILEM (1970). It is known for the comparatively simple setup and easy way of specimen production. According to Alvarez (1998), the determination of bond stress-slip relationships in pull-out tests is based on the notion that the pull-out body can reproduce the conditions at the infinitesimal bond element and that the influences of the test specimen and loading geometry are eliminated. The determined relationship would thus represent a kind of fundamental material law of bond, which could be modified in a further step to suit the conditions in real components. However, in reality the bond stress-slip relationship determined in the pull-out test is strongly dependent on the specific condition of the test specimen, and it is not possible to transfer these principles to the conditions in structural elements without further ado. The main weaknesses of the RILEM pull-out test are the large concrete cover and the arch effect of the reacting forces (Figure 1 left). This effect causes a transverse pressure in the bond zone, what increases the bond resistance and subsequently leads to an overestimation of the bearing capacity. Due to the minimum edge length of the test specimen of at least 200 mm or 10.0 times the bar diameter d_s, the minimum concrete cover is at least 90 mm, respectively $\geq 4.5 \cdot d_s$. The large concrete cover represents a high level of confinement and thus leads to a pull-out failure. For real structural elements, the concrete cover is usually in the range between 20 to 55 mm. Depending on the bar diameter, this normally corresponds to 1.0 to $4.0 \cdot d_s$. According to Vandewalle (1992), a concrete cover of 2.5 to $3.5 \cdot d_s$ is required to achieve a failure by bar pull-out.

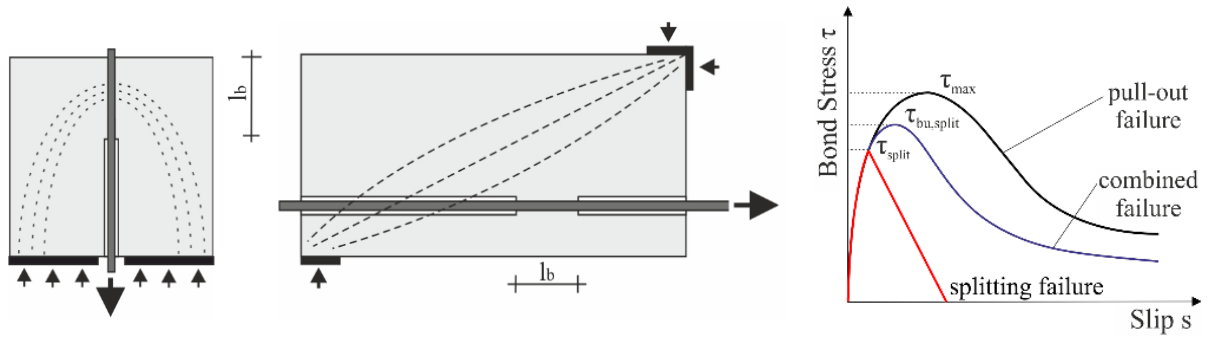

Figure 1. Schemes of pull-out test (left) and beam-end test (middle) and modes of bond failure (right)

In contrast, test configurations such as the beam test and the beam-end test (BE) represent the bond conditions of real RC components in a better way (Figure 1 middle). The force flow within the specimen does not cause any transverse stresses in the bond zone and the concrete cover is adjustable. Lower concrete

covers lead to a change of the failure mode towards a premature and more or less sudden splitting failure. Depending on the transverse reinforcement, both failure modes appear in combination (Figure 1 right), which may be defined as "splitting-induced pull-out failure". However, the associated guidelines and standards specify a bond length l_b of $10 \cdot d_s$ instead of $5 \cdot d_s$ in the pull-out test (see ASTM (2015) and RILEM (1970)). The comparison of results of bond tests with differently specified specimen types therefore includes the influence of different bond lengths.

The decrease in the length-related bond resistance τ_{ult} with increasing bond length was determined for plain bars by Bach (1905) and later confirmed by Mains (1951) for ribbed bars. By means of strain gauges distributed along the pull-out bar of long test specimens, Mains could reveal the non-uniform distribution of bond stresses for different load levels. From there on, bond tests with short bond lengths are preferred to determine the magnitude of the local bond stress maximum and the slip at which it occurs. For the definition of a short bond length the magnitude of $l_b \leq 5 \cdot d_s$ has been established in scientific practice. There are numerous bond models for the analytical description of the bond behaviour. The best known is that of the *fib* Model Code 2010 (2012), which is based on results of 125 pull-out tests with a bond length $l_b = 5 \cdot d_s$ and two normal strength concretes. In contrast to this, the investigations of Huang et al. (1996) revealed much higher bond stresses than expected by the bond model of MC2010. Based on their results of 28 pull-out tests with a bond length of $2.5 \cdot d_s$, they introduced a linear approach to describe the maximal bond stress in case of pull-out failure for normal and high strength concrete. Figure 2 shows the equations and parameters of both models for good bond conditions and well confined concrete.

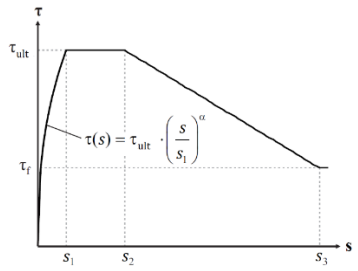

$$\tau(s) = \begin{cases} \tau_{ult} \cdot (s/s_1)^{\alpha}; & s \leq s_1 \\ \tau_{ult} & s_1 < s \leq s_2 \\ \tau_{ult} - (\tau_{ult} - \tau_f) \cdot \left(\frac{s - s_2}{s_3 - s_2}\right) & s_2 < s \leq s_3 \\ \tau_f & s_3 < s \end{cases}$$

Parameter	MC2010	Huang et al.	
		NSC	HSC
s_1 [mm]	1.0	1.0	0.5
s_2 [mm]	3.0	3.0	1.5
s_3 [mm]	c_{li}	c_{li}	c_{li}
α	0.4	0.4	0.3
τ_{ult}	$2.5 \cdot \sqrt{f_{cm}}$	$0.45 \cdot f_{cm}$	$0.45 \cdot f_{cm}$
τ_f/τ_{ult}	0.40	0.40	0.40

Figure 2. Models of the local bond-slip relationships by fib (2012) and Huang et a. (1996)

For few years now, distributed optical fiber sensing (DOFS) is offering the possibility of quasi-continuous measurement of strain values at intervals of less than one millimeter. DOFS have already been successfully applied in reinforced concrete for crack detection, strain measurements in concrete and as well at bond tests (Zdanowicz et al. 2022). Based on the local resolution of the strain along an embedded steel bar, conclusions can thus be drawn about the force transmission between reinforcement and concrete.

Bond Behaviour and crack development under long-term loading

Due to the load-dependent long-term behaviour of concrete, the high local compressive stresses in the area in front of the ribs lead to a change in the bond stress distribution and to increasing slip in bond tests over time. The effect of bond creep was investigated by Franke (1976) on normal and synthetic resin concrete specimens and by Rohling (1987) on the basis of different configurations of the pull-out specimens. Both came to the conclusion that a load-independent creep function can be assumed approximately for long-term loads at load levels up to about 50% of the short-term strength. According to Franke, the creep deformation can be calculated with equation 2, where $s_{t,0}$ is the initial slip at the beginning of the loading and t is the load duration in hours. This approach is also included in fib Model Code 2010 (2012).

$$s_t = s_{t,0} \cdot (1 + 10 \cdot t)^{0.080} \tag{2}$$

Rohling calculated a crack width increase of 40 to 48% under a permanent loading after 100,000 hours (about 11.4 years) using the bond-oriented crack theory of Krips (1985). The input parameters for these calculations were derived from the results of pull-out tests with a bond length of $5 \cdot d_s$. However, Rohling points out, that the quality of these calculations depends on how accurately the local bond law represents the actual conditions in the structural element. The rheological model by Empelmann and Cramer (2019) considers the time-dependent effects of concrete creep, shrinkage and bond creep separately. Based on their calculations for completed cracking, they conclude that bond creep leads to an increase in steel stresses in the area between cracks, while concrete stresses are reduced. As a consequence of these effects, they calculated a crack width growth of approx. 12% after 10,000 days (about 27.4 years). If concrete creep and shrinkage is also taking into account, they calculated an increase of about 33%. For their theoretical investigations, they used the bond stress-slip relationship of MC2010 (2012), which, however, does not take into account the influence of the bond length on the slip. Furthermore, only very few long-term tests with crack width measurements are available in the literature. To validate their calculations, Empelmann and Cramer used the experimental results of Jaccoud and Charif (1986). They tested two tension tie specimens with a constant load corresponding to a steel stress of 325 or 400 MPa over a period of 370 days. These loading rates resulted in two and eight cracks, whose width increased by approx. 30 and 20% during the test period.

EXPERIMENTAL METHODS

General and test program

The main aim of the investigations is to find a local bond relationship that is valid for the shortest possible bond length and thus provides a basis for calculations for long bond lengths and crack widths. The distribution of the bond stress along the bar is essential for this. To obtain this information, DOFS are applied to the pull-out bar for various bond length. The test program includes static tests with different bond lengths as reference and tests with long-term loading (Table 1). The purpose of these experiments is to explore how bond creep affects the distribution of strains and slip growth. Furthermore, these tests are to be used to draw conclusions about the crack width development under long-term loading.

Table 1: Number of tests per configuration (long-term tests in brackets; preliminary tests italic)

Type of concrete	**Test type**	**Bond length l_b in d_s**							
		1	**2**	**3**	**4**	**5**	**7,5**	**10**	**60**
C20/25	PO		3(3)			3(3)		3(3)	
	BE		3(3)			3(3)		3(3)	
	TT								(4)
C35/45	PO	4	3(3)	*24*+3	3	3(3)	3	3(3)	
	BE	4	3(3)	3	3	3(3)	3	3(3)	
	TT								(6)
C50/60	PO		3(3)			3(3)		3(3)	
	BE		3(3)			3(3)		3(3)	
	TT								(4)

Experimental investigations of bond behavior are performed with pull-out tests (PO) and beam-end tests (BE) for bond lengths from l_b = 1 to 10 times of the bar diameter d_s. In addition, the crack width development under long-term loading is investigated on tension tie specimens (TT) with an embedment length of $60 \cdot d_s$. Three normal strength concretes with the classes C20/25, C35/45 and C50/60 are tested in connection with Ø16 reinforcing bars made of BSt 500B (f_{yk} = 500 MPa). Most of the bond tests to date

have been carried out with the C35/45 after a minimum age of 56 days. With the C20/25 concrete, only the tests with a bond length $l_b = 2 \cdot d_s$ and two tension ties specimens were conducted so far. Some material tests were conducted with an age of 28 days, but revealed very little differences to the results of older samples. Table 2 shows the mean concrete properties with an age range of 28 to 224 days and the quantity of material tests.

Table 2: Concrete properties in MPa and quantity of tests (Number of tests in brackets)

Concrete	$f_{c,cube100}$	$f_{c,cyl}$	$f_{ct,sp,cube100}$	$f_{ct,fl}$	f_{ct}	$f_{ct}/f_{c,cyl}$	E_{cm}
C20/25	31.7 (14)	29.3 (9)	3.0 (9)	3.3 (6)	2.7 (6)	9.2%	31300 (6)
C35/45	67.3 (68)	54.7 (9)	4.4 (41)	4.9 (6)	3.3 (6)	6.0%	38700 (9)

The pull-out tests are configured according to the specifications by RILEM (1970) with 200 mm cubes and a cover of 92 mm ($c = 5.75 \cdot d_s$), but with a lead length of 80 mm and the different bond lengths as mentioned. Unlike the pull-out test, there is no defined standard for the beam-end test and the specimen's dimensions. The ASTM Guideline A944-10 (2015) provides some guidance on the principles of this test setup, but recommends dimensions that are inappropriate for the specific purpose of this examination. The used beam-end specimen was designed in dependence on the guideline, but was also modified. The chosen geometry for a bond length of $l_b = 3 \cdot d_s$ is shown in Figure 3.

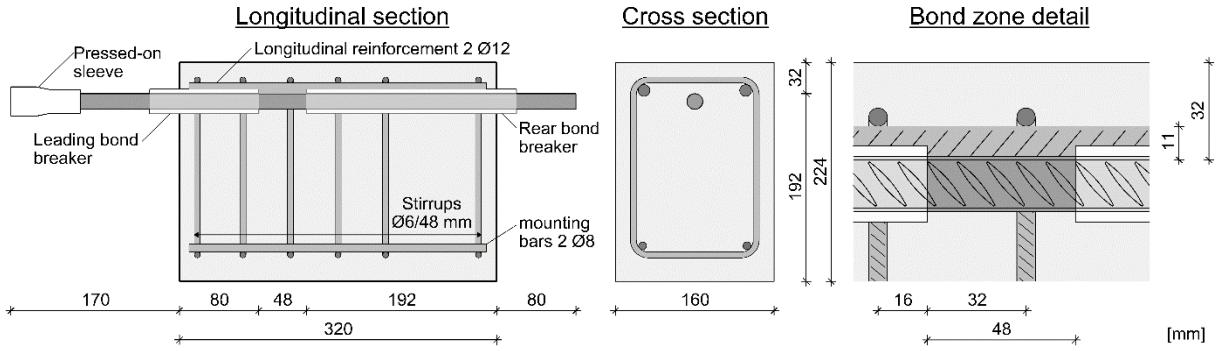

Figure 3. Configuration of beam-end specimen for a bond length $l_b = 3 \cdot d_s$

Plastic tubes with Ø25 mm are used to adjust the bond length. The concrete cover was set to $2 \cdot d_s$ or 32 mm, what is within the range of construction practice range. To prevent a sudden failure due to splitting, transverse reinforcement in the form of Ø6 stirrups with a spacing of 48 mm, respectively $A_{sv}/(s_v \cdot d_s) = 3.7\%$, is placed around the bond zone. In addition, the arrangement of the ribs starts always with the beginning of an inclined rib, shown in the bond zone detail of Figure 3. The tension tie specimens have a length of 960 mm and a square cross-section with the reinforcement bar in the centre. The influence of the concrete cover on the crack spacing is investigated through the different edge lengths 5, 7 and $9 \cdot d_s$. The specimens are usually made in series of 6 samples out of the same batch. The bar is placed in horizontal position during casting and the beam-end specimens are concreted upside-down to ensure good bonding conditions. After demolding the samples are covered with moist cloths for 6 days and then stored indoor until testing.

Instrumentation and test procedure

By default, for PO and BE tests, the slip at the unloaded end of the bar is measured by contact-free displacement transducers (LVDT). For static beam-end tests another LVDT is attached at the loaded end and two more LVDTs are placed right above the bond zone, one longitudinal and one in transverse direction,

to record the growth of cracks on the upper surface. The measurement distance is 100 mm for both of them. The force is measured with a load cell, which is connected with the hydraulic cylinder in case of monotonic loading. All static tests are performed path-controlled until a displacement of 10 mm. The signals were sampled with a rate of 5 Hz.

For the long-term tests, the specimens are loaded with 66% of the static bond strength, but not more than 66 kN. This value corresponds approximately to the stress level at full utilisation of the design strength of a Ø16 reinforcement bar or a steel stress σ_s = 330 MPa. The loading duration of the tests is usually 1000 h, for some tests 2000 h. To maintain the load for 1000 to 3000 h, a stack of disc springs is compressed with a hydraulic jack and the applied spring displacement is locked by a nut. In order to ensure a more or less constant loading, it is important for this test setup that the spring stroke is as large as possible so that the increasing slip over time does not cause any significant relaxation of the disc springs. To record any changes, a ring load cell is located between locking plate and nut. Figure 4 shows the experimental setup for the long-term tests.

Figure 4. Experimental setups for the long-term tests, PO (left), BE (middle) and TT (right)

Additionally distributed fibre optic sensors are used in all tests. These are mainly applied to the pull-out bar in order to record its strain distribution within the bond zone. Within the scope of a work package, the suitability of different sensor types and application locations on the bar was investigated. As a conclusion of these test series and the findings of other researchers (Bado et al. (2020)), a polyimide-coated sensor fibre is placed in grooves (1 by 1 mm) along the both longitudinal ribs of the bars. Thereby, the fibre is redirected once, so that it passes through the bond zone twice. The sensors are attached to the bars with cyanoacrylate and protected from interference by the concrete with a thin layer of silicone. In further tension tie tests, it is planned to apply DFOS also to the concrete surface in order to determine the crack widths. The measuring resolution is set to 0.65 mm and the sampling rate is 5 Hz.

RESULTS

Monotonic loading

So far, PO and BE tests have been carried out for the two concretes C20 and C35 with bond lengths l_b = 2 and 5·d_s, and for C35 also with l_b = 10·d_s. However, at this bond length, the PO tests were stopped at 130 kN, because the bar had almost reached the tensile strength without any significant increase in slip. Therefore, only the results of the other two bond lengths will be discussed in the following. The values for pull out force and slip determined in the monotonously loaded tests serve as a reference for the long-term tests. Table 3 gives an overview of these results.

Table 3: Mean values for tests under monotonic and long-term loading

Configuration				Monotonic loading				Long-term loading		
Measured variable			*calc.* f_{cm}	$\tau_{0.10}$	τ_{ult}	F_{ult}	$s_{0,ult}$	$F_{long\text{-}term}$	$s_{0,t=0}$	$s_{0,t=1000}$
Concrete	l_b	Test	[MPa]	[MPa]	[MPa]	[kN]	[mm]	[kN]	[mm]	[mm]
C20	$2{\cdot}d_s$	PO	27.5	7.4	15.2	24.4	0.96	16.4	0.42	1.10
		BE	31.1	8.15	16.0	25.7	0.84	17.5	0.19	0.48
	$5{\cdot}d_s$	PO	29.4	5.5	12.3	49.6	1.22	33.0	-	-
		BE	29.4	8.5	12.5	50.1	0.58	33.0	-	-
C35	$2{\cdot}d_s$	PO	49.4	14.9	28.9	46.4	1.13	31.0	0.16	0.45
		BE	57.0	21.9	28.1	45.1	0.42	30.5	0.06	0.21
	$5{\cdot}d_s$	PO	60.9	16.8	30.6	123.1	1.15	65.5	0.10	0.25
		BE	52.2	15.5	18.9	76.1	0.46	49.2	0.04	0.14

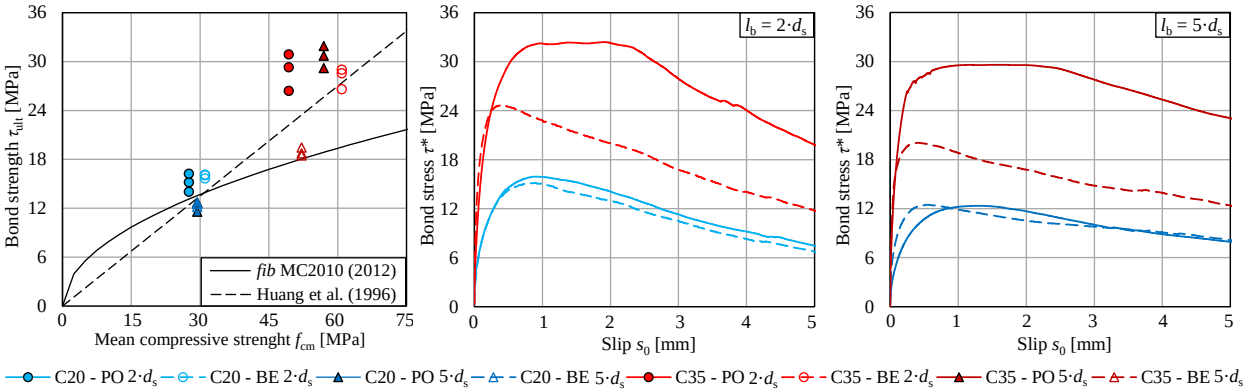

Figure 5. Relation of bond strength τ_{ult} to compressive strength f_{cm} (left), average curves of bond stress-slip relationships $l_b = 2{\cdot}d_s$ (middle) and $l_b = 5{\cdot}d_s$ (right); τ_* = bond stress in respect to the average strength for each concrete

Figure 5 left shows the bond strength τ_{ult} in respect to the mean compressive strength f_{cm}. Looking first at the influence of the concrete type, it becomes obvious that the bond resistance increases with the concrete strength. With the exception of the BE tests with $l_b = 5{\cdot}d_s$, the relationship between the two values is well represented by the linear approach of Huang et al. (1996). On the other hand, the approach according to MC2010 underestimates the bond strength for the C35. To draw further comparisons, the average bond stress-slip curves were related to respective average concrete strengths (Table 2) using the approach according to Huang et al. for both concrete grades. Comparing the specimen types, there is no significant difference between the results from PO and BE setups for the C20 for both bond lengths (see Figure 5 middle and right). For the C35, on the other hand, 25 to 33% lower bond strengths were determined with the BE setup compared to the PO tests. The reason for the different behaviour is most likely due to the higher relative tensile strength of the C20 (Table 2), which leads to a higher relative confinement effect. Regardless of the concrete type, higher $\tau_{0.10}$ in values were measured with the BE tests. This means a higher bond stiffness in the ascending branch (see i.e., Figure 5 right). The increase in bond length is accompanied by a reduction in bond strength for all configurations. This shows that for a bond length of $l_b = 5{\cdot}d_s$, the distribution of bond stress is not uniform and thus does not adequately represent the local bond behaviour. The decrease is particularly significant with approx. 20% in the BE-test for both concretes. The reason for this is probably the higher absolute pull-out forces for the longer bond length, which increases the splitting effect and lead to larger crack widths in BE specimens. In other words, the selected BE configuration has a certain resistance to splitting and crack growth independent of the bond length. Therefore, statements about the performance of PO and BE tests must always be made under consideration of the bond length.

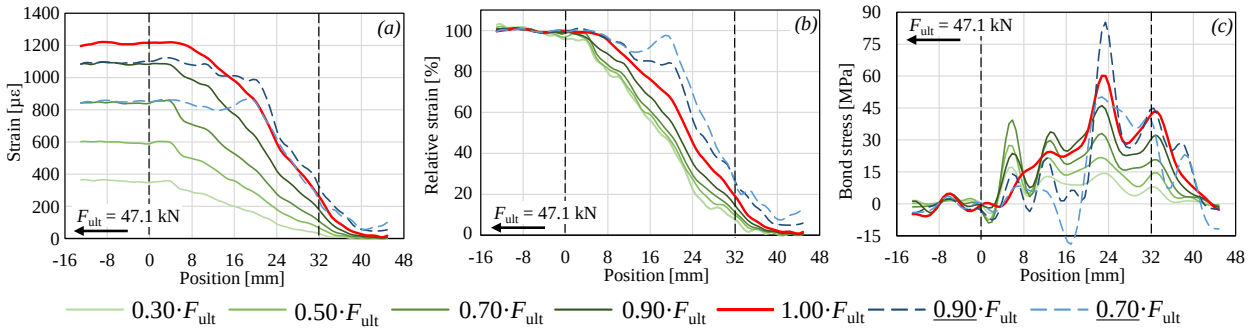

Figure 6. Strain distribution for different load levels (a), relative strain distribution (b) and bond stress distribution along bond length (c)

Information about the internal force transfer is provided by the DOFS recordings. Figure 6 (a) shows the mean steel strain distribution of both ribs along the bar within the bond zone and outside of it for a bond length l_b = 32 mm (2·d_s). If the measured values of different load levels are related to the corresponding strain before the bond zone, relative strain curves are obtained (Figure 9 b). It can be seen that the strain distribution changes with increasing load. Hence, there is a redistribution of bond stress. By local derivation of the strain curves and multiplication with d_s·E_s/4, the bond stress distributions for different load levels are obtained (Figure 6 c). In this curves, the individual four steel ribs of the bar can be identified due to local peaks, which appear more clearly with load increase. At 0.90·F_{ult}, the front peak begins to decrease, which is equivalent to the failure of the first concrete key. At the time of maximum loading F_{ult}, also the second concrete key started to collapse and the force is transmitted mainly by the two rear ribs. Further increase of the slip results in local bond stress of almost 90 MPa in front of the third inclined rib.

Bond under long-term loading

After carrying out the static tests, further samples of the same batch were subjected to a permanent load under indoor conditions between 18 and 24 °C. Out of the 18 long-term tests carried out so far, only one sample failed prematurely after approx. 7 h due to pull-out of the bar. It can be assumed that the bond resistance was reduced due to insufficient compaction. Figure 7 left shows the slip development for the bond length l_b = 2·d_s.

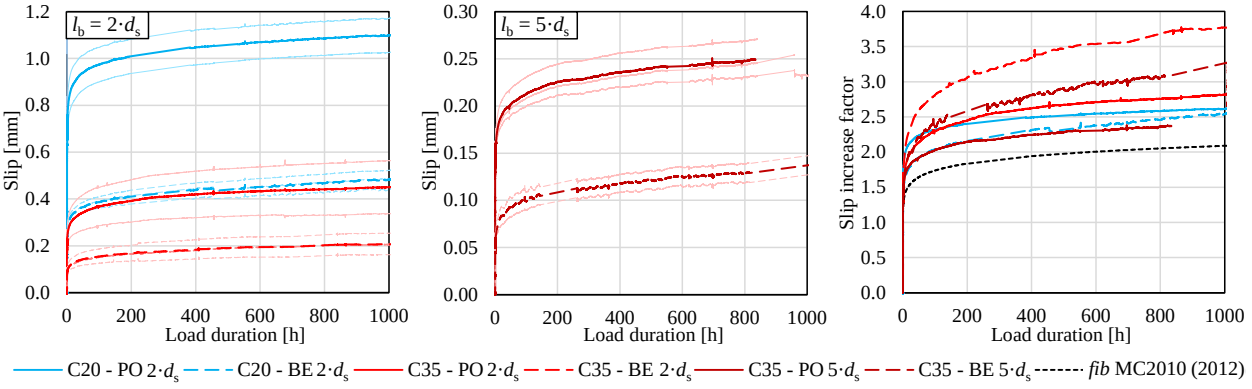

Figure 7. Slip increase under long-term loading for bond length l_b = 2·d_s (left) and l_b = 5·d_s (middle) and slip increase factor for different configuration (right)

First of all, it can be observed that lower slip values were recorded with the C35 than with the C20 for both test setups. The reason for this is probably the lower stiffness of the concrete C20 (see Table 2). Furthermore, it is remarkable that the PO tests already have larger slip values $s_{0,t=0}$ at the time of initial loading than the corresponding BE tests (see Table 3). With these, only about half the slip was recorded over the load duration than with the PO setup. The same phenomenon was also observed with the bond length $l_b = 5 \cdot d_s$ (Figure 7 middle). The reason for this specimen-related behaviour needs further investigation.

Figure 7 right shows the slip increase related to the initial slip $s_{0,t=0}$ for the tested configurations. After 1000 h of loading, an increase in slip by a factor of 2.5 to 3.7 was observed. There is no clear trend with regard to the test setup. However, less slip growth was measured with the C20 than with the C35. Furthermore, greater increases were achieved with the short bond length than with $l_b = 5 \cdot d_s$. The reason for this could be the intensified stress concentration on the first ribs for $l_b = 2 \cdot d_s$. The higher stress leads to bigger creep in these areas. Anyway, the approach according to MC2010 underestimates the slip growth under sustained loading for all test configurations by about 20 to 45%. Based on the results, the exponent is 0.12 on average, which is 1.5 times the value from MC2010 (see Equation 2).

Crack width growth under long-term loading

The crack width growth under permanent loading has been evaluated so far on two tension tie specimens with a cross-section of 80x80 mm and the concrete C35. The samples were subjected to a load of about 66 kN, respectively a steel stress of 330 MPa. During load application, 8 cracks with a mean crack spacing of approx. 10 cm appeared successively on both specimens, although these were not visible on all outer surfaces (Figure 8). This means that the introduction length is only about $l_t \approx 3 \cdot d_s$. However, tested samples with an edge length of 112 mm and thus doubling of the cross-section showed only 4 or 5 cracks with correspondingly large spacings.

Figure 8. Tension tie specimen with characteristic crack pattern

The crack growth was recorded by means of digital image correlation. At the beginning of loading, an average crack width of $w_{t=0} = 0.20$ mm was determined for both samples. After 1000 h an increase of 20% to $w_{t=1000} = 0.25$ mm was recorded. This development is mainly due to the small cracks, whose width nearly doubled, whereas no significant changes were measured for crack widths of 0.30 mm. Furthermore, 80% of the crack growth occurred in the first 10 hours and only 20% during the rest of the loading period.

CONCLUSION AND OUTLOOK

In this article, recent investigations about the local bond behaviour and crack width propagation of reinforced concrete under long-term loading were presented. The test programme with approx. 170 individual tests on three bond specimen types, the measurement concept and the test procedure are described. Through the systematic investigation of different bond lengths and the targeted use of DOFS, information about the force transfer within the bond zone is obtained. The results of the first tests seres on two normal strength concretes show that even with a bond length of $l_b = 2 \cdot d_s$, the force is not transmitted uniformly from the bar to the concrete and the bond behaviour depends strongly on the test setup. After 1000 h load duration, an increase in slip by a factor of 2.5 to 3.7 compared to the initial slip was observed as a result of creep under sustainable loading. In pull-out tests, the slip values measured were usually twice as big as in beam-end tests. However, all test results exceed the approach according to fib Model Code 2010

(2012) by 20 to 45%. Additionally tensile tie specimens were used to determine an increase in crack width of 20% compared to the beginning of the loading. Further investigations will deal with the evaluation of the recorded strain readings of DOFS and additional test series for another concrete.

ACKNOWLEDGEMENT

The presented studies are funded by the German Federal Ministry of Economic Affairs and Climate Action (BMWK, project No. 1501601) on basis of a decision by the German Bundestag. In addition, a thank goes to the Otto-Mohr-Laboratory for carrying out the test and the good cooperation.

REFERENCES

Alvarez, M. (1998). *Einfluss des Verbundverhaltens auf das Verformungsvermögen von Stahlbeton*. Doctoral Thesis, Eidgenössische Technische Hochschule Zürich, IBK Bericht 236

ASTM (2015). *A944-10 Standard test method for comparing bond strength of steel reinforcing bars to concrete using beam-end specimens*, ASTM international, West Conshohocken, USA.

Bach, C. (1905). "Versuche über den Gleitwiderstand einbetonierten Eisens," Mitteilungen über Forschungsarbeiten, 22 1–41.

Bado, M. F., Casas, J. R., Dey, A., Berrocal, C. G. (2020). "Distributed Optical Fiber Sensing Bonding Techniques Performance for Embedment inside Reinforced Concrete Structures", *Sensors*, 20 (5788) 1–23, doi:10.3390/s20205788.

BASE (2019). *Zwischenlager für hochradioaktive Abfälle – Sicherheit bis zur Endlagerung.* Bundesamt für die Sicherheit der nuklearen Entsorgung, Berlin

BMWi (2018). *7. Energieforschungsprogramm der Bundesregierung.* Bundesministerium für Wirtschaft, Berlin

Empelmann, M., Cramer, J. (2019). „Modell zur Beschreibung der zeitabhängigen Rissbreitenentwicklung in Stahlbetonbauteilen," *Beton- und Stahlbetonbau*, Germany, 114(5) 327–336.

fib Bulletin 65 (2012). *Model Code 2010 – Final draft, Volume 1.* Federation international du béton (fib), Lausanne

Franke, L. (1976). "Einfluß der Belastungsdauer auf das Verbundverhalten von Stahl und Beton (Verbundkriechen)," Deutscher Ausschuss für Stahlbeton (Eds.): Vol. 268, Beuth Verlag, Berlin

Jaccoud, J.-P., Charif, H. (1986). *Armanture minimale pour le contrôle de la fissureation: rapport final des essais série C,* Publication IBAP no. 114, Ecole Polytechnique Fédérale des Lausanne

Krips, M. (1985). "Rißbreitenbeschränkung im Stahlbeton und Spannbeton," Doctor Thesis, Technische Hochschule Darmstadt.

Lindorf, A. (2011). *Ermüdung des Verbundes von Stahlbeton unter Querzug.* Doctoral Thesis, Technische Universität Dresden.

Mains, R. M. (1951). "Measurement of the distribution of tensile and bond stresses along reinforcing bars," *Journal of the American Concrete Institute*, USA, 23 225–252.

RILEM (1970). „Essais portant sur l'adhérence des armatures du béton," *Matériaux et Constructions*, France, 3 169–178.

Rohling, A. (1987). *Zum Einfluss des Verbundskriechens auf die Rissbreitenentwicklung sowie auf die Mitwirkung des Betons auf Zug zwischen den Rissen.* Doctoral Thesis, Technische Universität Braunschweig

Vandevalle, L. (1992). "Theoretical prediction of the ultimate bond strength between a reinforcement bar and concrete," *Proc., Bond in concrete: International conference bond in concrete from research to practice*, Vol. 1, Riga, Latvia, 1/1-1/8

Zdanowicz, K., Gebauer, D., Koschemann, M., Speck, K., Steinbock, O., Beckmann, B., Marx, S. (2022). "Distributed fibre optic sensors for measuring strains of concrete, steel and textile reinforcement: Possible fields of application," *Structural Concrete*. 1-16, DOI: 10.1002/suco.202100689